Estimation of Ship Roll Damping - a Comparison of the Decay and the Harmonic Excited Roll Motion Technique for a Post Panamax Container Ship

Sven Handschel, *TU Hamburg-Harburg*, sven.handschel@tuhh.de

Dag-Frederik Feder, *TU Hamburg-Harburg*, dag.feder@tuhh.de

Moustafa Abdel-Maksoud, *TU Hamburg-Harburg*, m.abdel-maksoud@tuhh.de

ABSTRACT

The decay motion as well as the harmonic excited roll motion are established techniques to estimate roll damping for ships. This paper compares the advantages and disadvantages of both techniques and focuses on their applicability. Different analysis methods for both techniques to determine the nonlinear roll damping moment are investigated with the aim of developing an exact estimation approach without additional filtering, curve fitting and offset manipulation of the recorded time series. Damping coefficients of both techniques are compared for available experiments of the benchmarking post panamax container ship model Duisburg Test Case (DTC). Reasons for deviations are investigated, and the influence of an accurate estimation of the current nonlinear hydrostatic moment will be shown. In this context, the experimental estimation is more convenient than an additional calculation. A method for the determination of the nonlinear hydrostatic moment during a harmonic excited roll motion test is presented. Different approximations of roll damping based on series expansion are investigated. Disadvantages of a widely used approach are discussed based on the results.

Keywords: *roll damping, decay technique, harmonic excited roll motion technique*

1. INTRODUCTION

Boundary element methods (BEM) based on the potential theory can, in most cases, simulate ship motions with sufficient accuracy. They are accurate enough for many applications, and compared to finite volume methods (FVM), they are computationally efficient. Ship motions are mainly damped by the generation of surface waves which radiate from the ship. This is not valid for the roll motion. The roll motion is influenced by additional damping effects which cannot be predicted by BEMs. To consider these effects, roll damping is often estimated separately. Hence different techniques exist. Common techniques are (I) the roll decay (see e.g. Spouge, 1988), (II) the harmonic excited roll motion (called HERM, see Sugai et al., 1963, Blume, 1979 and Handschel et al., 2014a) and (III) the harmonic forced roll motion (Bassler et al., 2010 and Handschel et al. 2014b), see also Figure 1. Techniques (I) and (II) estimate the roll damping moment from the roll angle recording. In technique (III) the roll moment is directly determined on a fixed predefined roll axis.

Applicability of the techniques: Table 1 shows a comparison of the properties of all three techniques. Only with the decay (I) and the harmonic excited roll motion technique (II) does the ship roll with a natural free motion axis. In fact, the fixed roll axis of technique (III) and the direct determination of the moment enable an easy validation process for numerical simulation methods (see also Handschel et al., 2014b), but the natural motion coupling of the degrees of freedom is suppressed. In this paper, technique (III) will not be further investigated.

Table 1 Advantages and disadvantages of techniques to estimate roll damping

* less/small *** high/large	(I)	(II)	(III)
Real motion coupling	yes	yes	no
Steady roll motion	no	possible	possible
Large roll amplitudes	*	***	***
Forward speed	*	***	***
Time and cost	*	**	***

In contrast to the harmonic excited roll motion technique (II), no roll damping for large roll amplitudes and forward velocities can be estimated by the decay technique (I). Large forward velocities are associated with large damping moments. The high roll damping prevents the realisation of sufficient numbers of roll periods with the decay technique, which are necessary to analyse roll damping with high accuracy. Nevertheless, the decay technique is a low cost technique and does not require much towing tank testing time.

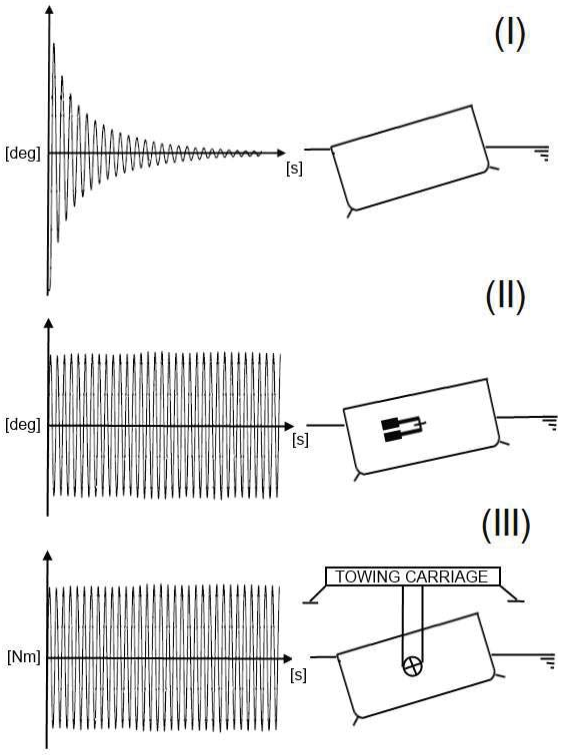

Figure 1 Techniques to estimate roll damping

Post panamax container ship: In the present paper model tests are included for the post panamax container ship Duisburg Test Case (DTC, Table 2, see el Moctar et al., 2012). The model is equipped with bilge keels, a propeller and a full spade rudder. The bilge keels are separated in five parts with a breadth of $0.008\,B_{WL}$. Especially the huge bow flare area as well as the transom stern is typical for this type of ship. The model tests were carried out for DTC with a full scale length of $L_{WL} = 361m$ in full loading condition at Hamburg ship model basin (HSVA, Schumacher, 2010). A scale factor of 59.467 is applied.

Table 2 Main dimensions Duisburg Test Case (DTC) for full loading and ballast condition – scale factor 1:59.467

	full loading	*ballast*
L_{WL}	6.0691 m	5.9391 m
B_{WL}	0.8576 m	0.8576 m
D	0.2354 m	0.2018 m
KG	0.3992 m	0.235 m
C_B	0.6544	0.6288
∇	0.7887 m^3	0.6496 m^3
i_{xx}	0.3967 B_{WL}	0.3801 B_{WL}
i_{yy}, i_{zz}	0.2447 L_{WL}	0.2713 L_{WL}

The paper presents results for both measurement techniques (I) and (II). Three different analysis methods based on a one degree of freedom, namely the roll motion equation, are investigated. The focus is set on identifying a method which determines roll damping without additional filtering [1] and curve fitting. The analysis methods should also work with typical measurement offsets which could be observed in the available roll angle

[1] It is assumed that the prior filtering of the signals with a measurement amplifier is weak.

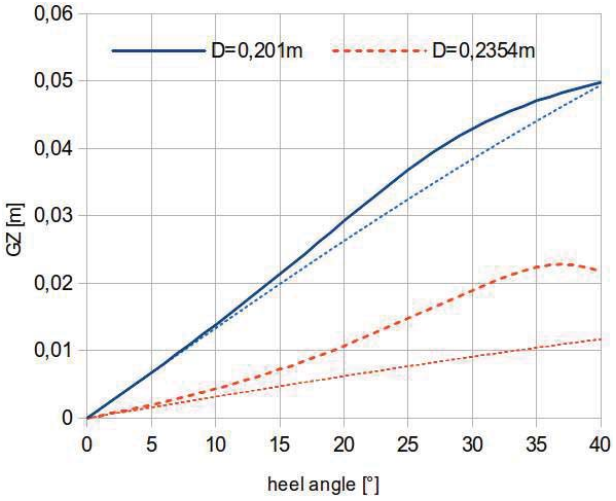

Figure 2 GZ curve DTC: full loading (red) and ballast condition (blue) / dotted line: linearization of hydrostatic moment

measurements. Furthermore, it will be shown that a comparison of the results for both techniques depends on an exact determination of the hydrostatic moment. For the application in ship motion simulations, damping coefficients are usually formulated as a linear, quadratic or as a cubic function of the roll velocity. The applicability of these approximations will be discussed. It will be shown that each approach can lead to certain deviations.

2. ROLL MOTION OF SHIPS

2.1 Equation of Roll Motion

Considering one degree of freedom, the roll equation can be formulated based on Newton's second law. The coefficients of the inertia moment of the ship M_φ, damping moment N_φ, restoring moment S_φ and the external moment F_φ are usually formulated with a balance between the rigid body moments and external moments:

$$M_\varphi \frac{\partial^2 \varphi}{\partial t^2} + N_\varphi \frac{\partial \varphi}{\partial t} + S_\varphi \varphi = F_\varphi(t). \tag{1}$$

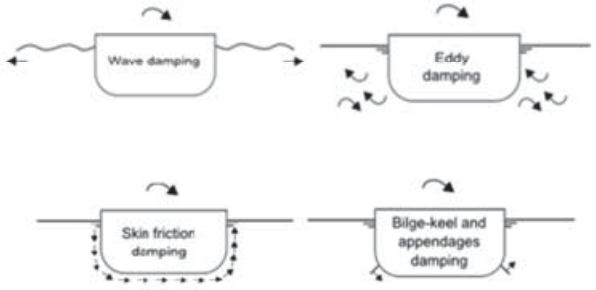

Figure 3 Separation of roll damping phenomena

The $GZ(\varphi_{heel})$-curve, the change of the lever arm over the heel angle, characterises the hydrostatic moment

$$S_\varphi(\varphi) = \frac{g\Delta GZ(\varphi)}{\varphi}. \tag{2}$$

It can be determined by static or dynamic measurements (see Section 4). Figure 2 includes the $GZ(\varphi_{heel})$-curves for both load cases.

The undamped natural frequency of the ship can be described by the ratio of the hydrostatic and inertia moment coefficients:

$$\omega_0 = \sqrt{\frac{S_\varphi}{M_\varphi}}. \tag{3}$$

From this equation, the total inertia, the sum of the ship inertia and the virtual inertia due to the acceleration of the fluid, can be determined exactly at the undamped natural frequency by

$$M_\varphi = \frac{g\Delta GZ(\varphi)}{\omega_0^{\,2}\varphi}. \tag{4}$$

2.2 Roll Damping

The roll damping moment N_φ is generated by wave radiation, vortex generation and the lift and friction on the hull (see Himeno, 1981 and

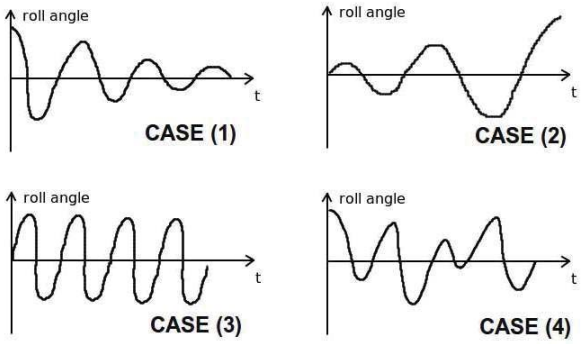

Figure 4 Rolling of ships in irregular waves

Figure 3[2]). In addition, ship appendages can have a noticeable effect on roll damping.

For the consideration of the total roll damping, additional damping terms are embedded in BEM simulation methods. These were usually estimated by the decay (I) or harmonic excited roll motion (HERM, II) technique via experiments or numerical simulations (see Sarkar, 2000, Salui, 2004, Röös, 2009, el Moctar et al., 2010, Gao et al., 2010, Handschel et al., 2012a).

Using an energy approach over one period,

$$E_E = 4\int_0^{\varphi_a} N_\varphi \dot{\varphi} d\varphi = \pi N_{\varphi e} \omega {\varphi_a}^2, \tag{5}$$

the damping moment can be expressed as an equivalent damping coefficient $N_{\varphi e}$ which depends on the roll frequency ω and the roll amplitude assuming harmonic behaviour $\varphi = \varphi_a \sin(\omega t)$. The equivalent non-dimensional roll damping coefficient B_φ is formulated according to the ITTC as

$$B_\varphi(\varphi_a) = \frac{N_{\varphi e}(\varphi_a)}{\rho \nabla {B_{WL}}^2} \sqrt{\frac{B_{WL}}{2g}}. \tag{6}$$

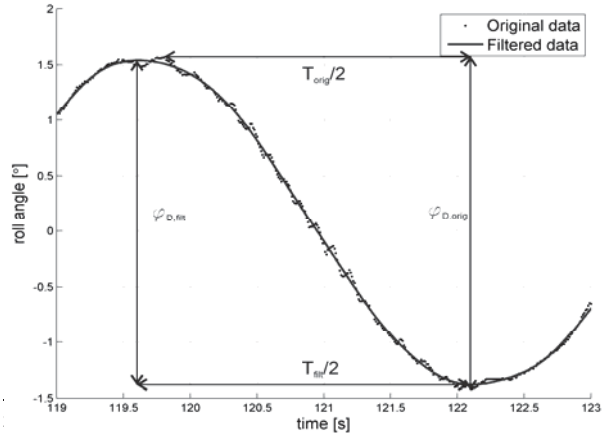

Figure 5 Comparison unfiltered and filtered signal

2.3 Roll Motion in Irregular Waves

The rolling of ships in irregular waves can be divided in four scenarios, see Figure 4: a roll motion with (1) a decreasing roll amplitude, (2) an increasing roll amplitude, (3) a constant roll amplitude and (4) an alternation of increasing and decreasing amplitudes. The variation of the roll amplitude depends mainly on the wave period and wave height.

A problem of the discussed techniques is that each of them considers only one of four scenarios. The decay motion (I) corresponds to the first case, HERMs (II) to case (3).

3. ESTIMATION OF ROLL DAMPING

3.1 Roll Decay Motion

Roll decay measurements are straight forward and can be easily realised. The ship is excited once and decayed to the rest position. The measured time series of the roll angle are analysed to estimate roll damping. Carried out in towing tanks, they are less expensive than other techniques.

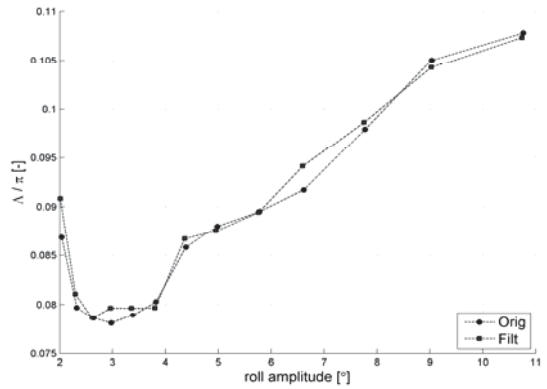

Figure 6 Comparison unfiltered and filtered results for logarithmic decrement – full loading condition, Fn=0.10

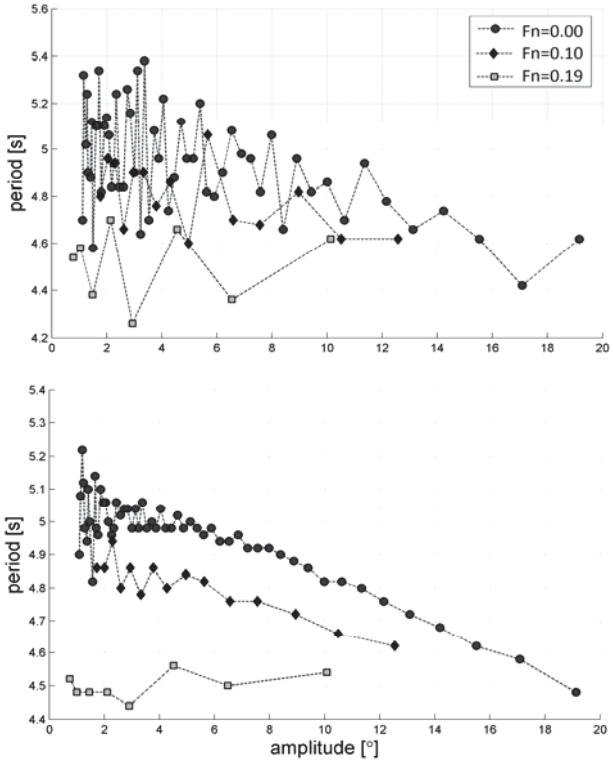

Figure 7 Comparison unfiltered (upper diagram) and filtered resonance roll period for full loading condition

Three methods (A, B and C) are investigated for the (D)ecay technique. Methods based on the logarithmic roll decrement (D.A) and energy conservation (D.B and D.C) are analysed. The roll motion occurs in the damped natural frequency

$$\omega_D = \omega_0 \sqrt{1 - \left(\frac{N_{\varphi e}}{2\omega_0 M_\varphi} \right)^2} \tag{7}$$

which is evaluated for every half period. The influence of low-pass filtering is investigated. The measurement window in Figure 5 shows an example of the filter application. The influence of noise on determining double amplitudes φ_D is not significant for the presented results, see Figure 6. Improvements can mainly be observed for determining the roll period $T = 2\pi / \omega_D$ from peak to peak (Figure 7).

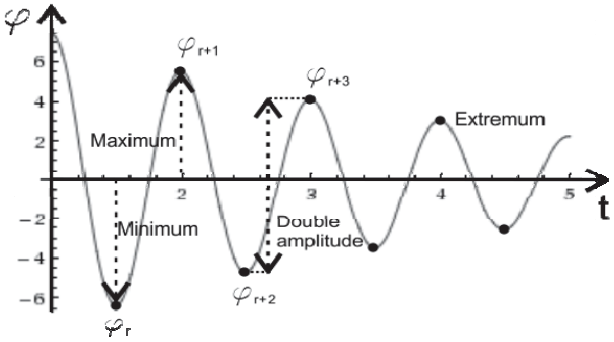

Figure 8 Decay test

Method (D.A): Four variations of the *logarithmic decrement* method

$$\Lambda = \frac{1}{j} \ln \frac{|\varphi(t)|}{|\varphi(t + j\frac{2\pi}{\omega})|} \tag{8}$$

are tested: with all extrema, only maxima or minima as well as double amplitudes, see Figure 8. Only the application of double amplitudes compensates for possible measurement offsets. The damping coefficient is defined as

$$N_{\varphi e}(\varphi_a) = \frac{M_\varphi \omega_D(\varphi_a)}{\pi} \ln \left(\frac{|\varphi_r - \varphi_{r+1}|}{|\varphi_{r+2} - \varphi_{r+3}|} \right) \tag{9}$$

for

$$\varphi_a = \left(\frac{|\varphi_r - \varphi_{r+1}| + |\varphi_{r+2} - \varphi_{r+3}|}{4} \right). \tag{10}$$

Method (D.B): The 'Froude'-energy method (see Spouge, 1988) is based on the energy conservation of the dissipated energy E_E and the – hydrostatic – *potential energy* $E_{D.B}$ in the roll maximum ($\dot{\varphi} = 0$):

$$E_{D.B} = g\Delta \int_{\varphi_D}^{\varphi_{D+1}} GZ(\varphi) d\varphi. \tag{11}$$

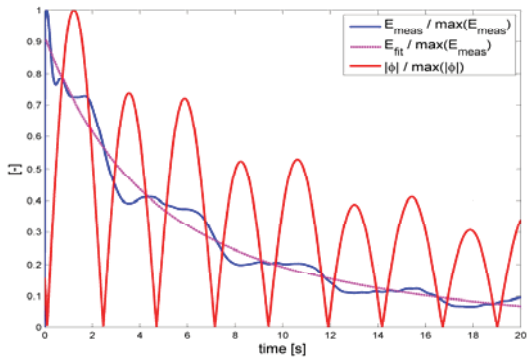

Figure 9 Curve fit (dotted, pink) of energy function (blue), Eq. (13) – full loading condition, Fn=0.10

Instead of using only extrema, it is more useful to formulate the method for double amplitudes φ_D to compensate for possible measurement offsets. Both energy formulations are equated ($E_E = E_{D.B}$), which results to

$$N_\varphi(\varphi_a) = \frac{E_{D,B}}{\pi \omega_D {\varphi_a}^2}. \qquad (12)$$

Method (D.C): This method (see Roberts, 1985 and Spouge, 1988) is also based on energy conservation, but for the sum of potential and kinetic energy. Instead of using an integral term as method (D.B), Roberts recommends a differential term to estimate the energy loss rate $dE_{D.C}/dt$. The energy equation is given by:

$$E_{D.C}(t) = \frac{1}{2}\dot{\varphi}^2 + \frac{1}{2}{\omega_D}^2 \varphi^2. \qquad (13)$$

In contrast to Spouge, 1988, who fitted the function $E_{D.C}$ by a cubic spline curve, in this investigation exponential functions are used, see Figure 9. The roll damping follows to

$$N_\varphi(\varphi_a) = -M_\varphi \left(\frac{dE_{D.C}}{dt} \right) / E_{D.C}. \qquad (14)$$

Applicability of method (A), (B) and (C): The methods presented can be used in the resonance frequency ω_D and for ships with linear or nonlinear righting arm curves. Table 3 shows an overview of advantages and disadvantages of each analysis method in the case of a decay motion. The focus was set on three points: (i) if a filtering of the roll angle time series is required, (ii) if a curve fitting is necessary for the analysis method and (iii) if a measurement offset of the roll angle leads to deviations of the results. The information given in Table 3 has been verified in a comparative study for an analytical decay function in the Appendix, Figure 17.

Unfortunately, with all methods, the time series have to be filtered3 to achieve satisfied results. Double amplitudes compensate for deviations due to measurement offsets in methods (D.A) and (D.B). Method (D.C) is able to estimate roll damping for larger amplitudes based on a curve fitting of the energy. It has to be mentioned that an approximation by curve fitting is a compromise between exactness and the possibility to estimate roll damping over a wider range of roll amplitudes.

Table 3 Advantages and disadvantages of the presented analysis methods for technique (I)

	(D.A)[4]	**(D.B)**	**(D.C)**
Filter required	yes	yes	yes
Curve fit required	no	no	yes
Sensitive to measurement offset	weak	weak	yes
# of peaks at start for which no result of N_φ can be estimated	2	2	0

3.2 Harmonic Excited Roll Motion

The (H)armonic roll motion corresponds to the third scenario (constant amplitude) of the roll motion in irregular waves, see Figure 4. The motion is excited by two contrary rotating weights (Blume, 1979) or by flying wheels

[3] Butterworth lowpass filter 8th-order with cuttoff frequency $\omega_C = 5\omega_D$.

[4] Logarithmic roll decrement method with double amplitudes.

(Sugai et al., 1963). Three different analysis methods are known which are independent from the roll resonance frequency. Details can be found in Handschel et al., 2014a.

The methods are all based on energy conservation over one roll period, see Eq. (5). The maximum roll amplitude, the peak, occurs at the frequency (see also Spouge, 1988)

$$\omega_P = \omega_0 \sqrt{1 - \frac{1}{2}\left(\frac{N_{\varphi e}}{\omega_0 M_\varphi}\right)^2} \tag{15}$$

for harmonic motion with sinusoidal excitation.

Method (H.A): The roll angle

$$\varphi(t) = \varphi_a \sin(\omega t + \vartheta) \tag{16}$$

is *phase-shifted by* ϑ with respect to the initiated roll moment, see Figure 10,

$$F_\varphi(t) = F_{\varphi,a} \sin(\omega t). \tag{17}$$

The work done by the exciting moment in one roll period is

$$E_{H.A} = \int_0^T F_\varphi \dot{\varphi} dt = F_{\varphi,a} \varphi_a \pi \sin\vartheta. \tag{18}$$

The dissipated damping energy and the work done by the exciting moment over one roll period should be the same. With the relation $E_E = E_{H.A}$ the equivalent roll damping can be calculated by:

$$N_\varphi(\varphi_a) = \frac{F_{\varphi,a} \sin\vartheta}{\omega \varphi_a}. \tag{19}$$

Method (H.B): The roll moment and roll angle span a closed trajectory in phase-space, a Lissajous curve (Figure 10). The area inside the

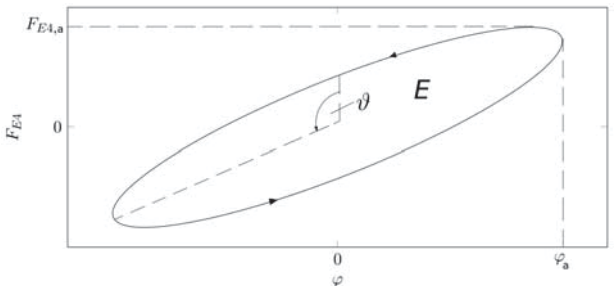

Figure 10 phase plot of the roll moment (here F_{E4}) and the excited roll angle, Lissajous curve

trajectory is the energy which dissipates over a roll period

$$E_{H.B} = \int_{\frac{-\pi}{\omega}}^{\frac{\pi}{\omega}} F_\varphi d\varphi \tag{20}$$

$$N_\varphi(\varphi_a) = \frac{E_B}{\pi \omega {\varphi_a}^2}. \tag{21}$$

Method (H.C): The analysis with the Fourier transform is based on the condition that only the damping moment is phase-shifted by 90° to the roll angle. A Fourier polynomial approximates the roll moment:

$$F_\varphi(t) = \sum_{k=1}^{\infty} \begin{pmatrix} C_{A,k} \\ C_{B,k} \end{pmatrix} \cdot \begin{pmatrix} \sin(k\omega t) \\ \cos(k\omega t) \end{pmatrix}, \tag{22}$$

which will be inserted in Equation (20).

$$E_{H.C} = \int_{\frac{-\pi}{\omega}}^{\frac{\pi}{\omega}} \sum_{k=1}^{\infty} \begin{pmatrix} C_{A,k} \\ C_{B,k} \end{pmatrix} \cdot \begin{pmatrix} \sin(k\omega t) \\ \cos(k\omega t) \end{pmatrix} d\varphi \tag{23}$$

$$E_{H.C} = \pi \varphi_a C_{B,1} \Rightarrow N_\varphi(\varphi_a) = \frac{C_{B,1}}{\omega \varphi_a} \tag{24}$$

Applicability of method (A), (B) and (C): The methods presented can be used for all frequencies ω and for ships with linear or nonlinear curves of righting arm. Table 4 shows an overview of advantages and disadvantages of each analysis method in the

case of *a harmonic roll motion with constant roll amplitude*. As an example a comparison of the non-dimensional damping coefficient for an analytical test case is given in Table 5 of the Appendix. It can be summarised that all three methods are very robust. A low-pass filter was not used for the presented case. Correct results can be obtained by method (H.A) for $\vartheta \to n\pi(n \in Z)$ when high sampling rate can be achieved. If the signal is overlapped by a strong background noise or has a low sampling rate, method (H.C) is recommended due to the robustness of the Fourier transform approach.

Table 4 Advantages and disadvantages of the presented analysis methods for technique (II)

	(H.A)	**(H.B)**	**(H.C)**
Filter required/used	no	no	no
Curve fit required	no	no	no
Sensitive to Measurement offset	weak	weak	weak
Sensitive to $\vartheta \to n\pi(n \in Z)$	yes	no	no

3.3 Comparison of both techniques

For a comparison of both techniques

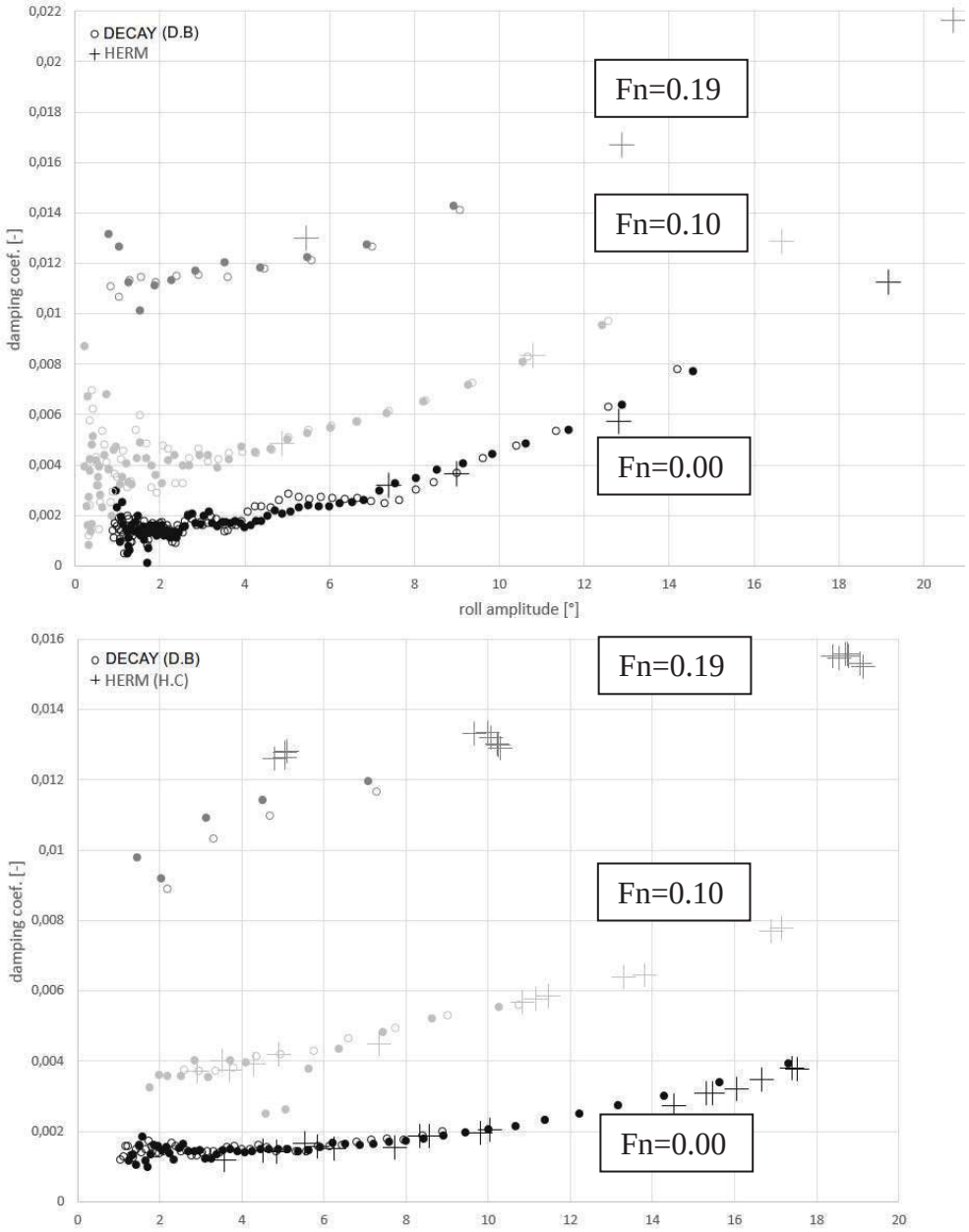

Figure 11 and 12 Comparison of data points with technique I (D.B) and technique II (H.C) for ballast (upper figure) and full loading condition (lower figure) - Fn=0.00 (black), Fn=0.10 (light grey), Fn=0.19 (grey)

methods (D.B) and (H.C) are selected. The decay measurement results have partially an offset. For this reason method (D.C) cannot be applied. To compare both experimental results, the non-dimensional formulation B_{φ} (see Eq. 6) is chosen. Compared to technique (II) where the moment is forced and known, a moment for technique (I) must be calculated. Therefore, besides the time series of the roll angle, the estimation of the roll inertia or roll hydrostatic moment is necessary to calculate the damping moment. In the present roll resonance frequency ω_D , the inertia and hydrostatic moment are equal. Because of the complexity in estimating the roll inertia moment, it is recommended to estimate the hydrostatic moment. Method (D.B) is based on this recommendation. The results for ballast and full loading conditions at Froude numbers 0.00, 0.10 and 0.19 are presented in Figures 11 and 12.

Deviations between both techniques (I) and (II) are mainly based on the different approaches to estimate damping and their realisation or uncertainties of the model tests and analysis errors.

- Deviations can be based on the different approaches. Technique (I) is similar to scenario case (1), technique (II) similar to case (3). These deviations cannot be prevented and are physically-based.

- Technique (II) is carried out with a steering rudder which holds the model on course in the narrow towing tank. Unfortunately, the influence of the rudder was not investigated. It should be expected that the rudder has an influence on the roll motion.

- To estimate roll damping by the decay technique (I), the righting arm curve has to be determined with high accuracy. To prevent deviations due to uncertainties of additional model tests or computations, it is recommended to determine the hydrostatic moment based on the existing decay or HERM measurements. Different aspects can influence the GZ-values compared to computational estimated values, e.g. the manufacturing accuracy of the model as well as the correct model setup due to large scale factors. Unfortunately, an effective approach to estimate the hydrostatic roll moment based on HERM model tests was developed after carrying out the tests with the DTC, see Section 4. For this reason, GZ-values can be evaluated for only a few roll amplitudes, see Figure 14.

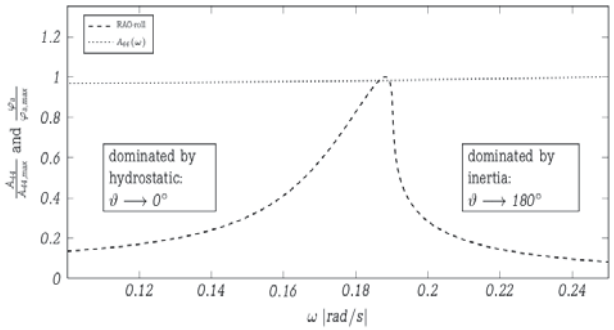

Figure 13 Sample Response Amplitude Operator (RAO) for the roll motion and virtual added inertia

4. DYNAMIC ESTIMATION OF HYDROSTATIC ROLL MOMENT

Two experimental techniques can be applied to estimate the lever arm GZ:

- A *static* technique – inclining tests with different weights and distances.

- A *dynamic* technique using HERM measurements.

Nearly all roll amplitudes occur twice: once in the frequency range dominated by the hydrostatic moment (ω_1) and once in the frequency range dominated by the inertia moment (ω_2), see Fig. 13 and Handschel et al., 2014a.

If the virtual added inertias of both frequencies are equated, this results to

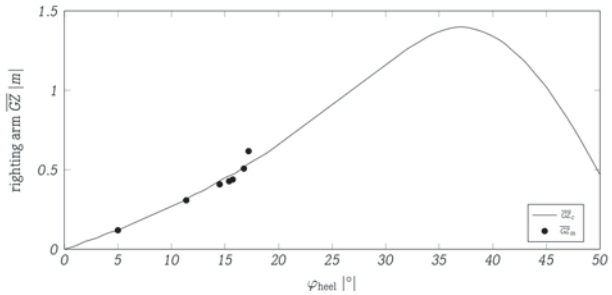

Figure 14 Estimation of the righting arms based on measurement results and calculated GZ-values (full scale)

$$\overline{GZ}(\varphi_a) = \frac{\omega_1^{\,2} X - c_\alpha \omega_2^{\,2} F_{\varphi,a} \cos\vartheta_1}{g\Delta\left(\omega_1^{\,2} - c_\alpha \omega_2^{\,2}\right)} \tag{25}$$

with

$$X = F_{\varphi,a} \cos\vartheta_2 - (c_\alpha - 1)\varphi_a \omega_2^{\,2} i_{xx}^{\,2} \Delta \tag{26}$$

and $c_\alpha = A_{\varphi,2} / A_{\varphi,1}$ the ratio of both virtual added inertia. If the virtual added inertia is equal for both frequencies, Equation (25) simplifies to

$$\overline{GZ}(\varphi_a) = \frac{\omega_1^{\,2} F_{\varphi,a} \cos\vartheta_2 - \omega_2^{\,2} F_{\varphi,a} \cos\vartheta_1}{g\Delta\left(\omega_1^{\,2} - \omega_2^{\,2}\right)}. \tag{27}$$

Figure 14 shows the differences between calculated GZ-values and measured values. Differences are up to 7% in the present case, see Handschel et al., 2014a.

5. IMPLEMENTATION OF ESTIMATED DAMPING MOMENTS IN SHIP MOTION SIMULATIONS

5.1 Frequency Domain

Although results of both techniques look similar, the estimation with the HERM (II) technique is recommended. In frequency domain, the roll motion is also simulated as a steady-state harmonic motion, scenario case (3), see Figure 4.

5.2 Time Domain – Series Expansion

Regardless of which technique is selected to estimate roll damping, usually a polynomial expansion of the roll velocity with linear, quadratic or cubic terms is used to approximate roll damping over various roll amplitudes (Spouge, 1988 and 26th ITTC, 2011).

$$N_\varphi \dot{\varphi} = N_{\varphi 1}\dot{\varphi} + N_{\varphi 2}\dot{\varphi}\,|\,\dot{\varphi}\,| + N_{\varphi 3}\dot{\varphi}^3 \tag{28}$$

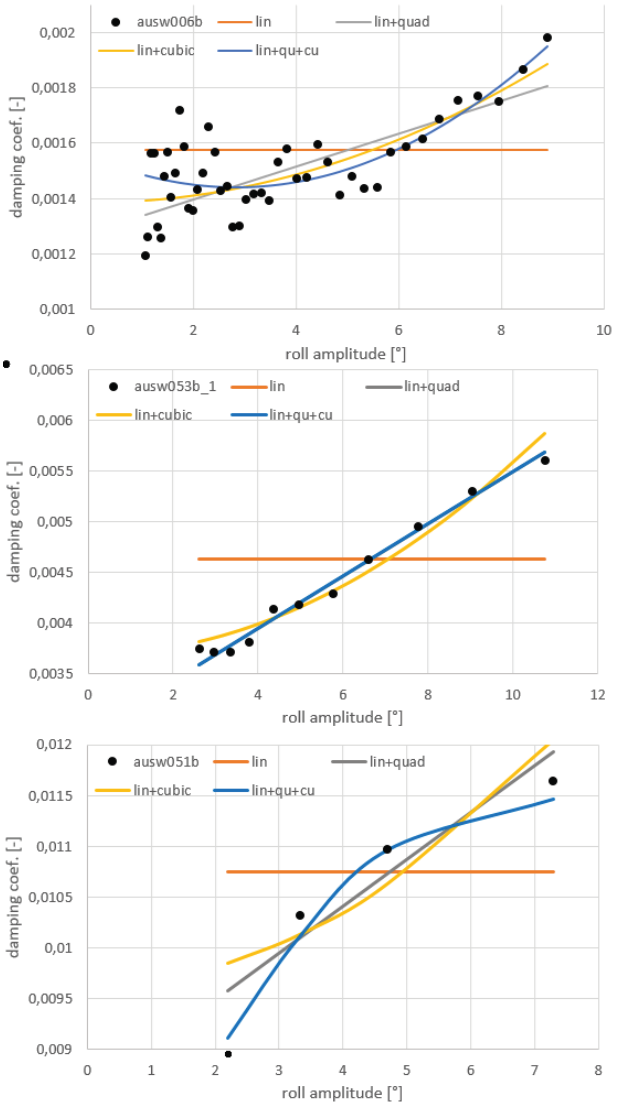

Figure 16 Different polynomials for data points of decay measurements with Fn=0.00 (upper), 0.10 and 0.19 (lowest)

A widley used approach is that different combinations of order of the polynomial expansions are included directly in the analysis methods (D) and (H), see Figure 15 - upper chart.

As an example, results for the full loading condition of the container ship DTC are fitted to a

- *linear:*
  $N_\varphi \dot{\varphi} = N_{\varphi\dot{\varphi}} \dot{\varphi}$,
- *linear+quadratic:*
  $N_\varphi \dot{\varphi} = N_{\varphi 1} \dot{\varphi} + N_{\varphi 2} \dot{\varphi} |\dot{\varphi}|$,
- *linear+cubic:*
  $N_\varphi \dot{\varphi} = N_{\varphi 1} \dot{\varphi} + N_{\varphi 3} \dot{\varphi}^3$
- and *linear+quadratic+cubic:*
  $N_\varphi \dot{\varphi} = N_{\varphi 1} \dot{\varphi} + N_{\varphi 2} \dot{\varphi} |\dot{\varphi}| + N_{\varphi 3} \dot{\varphi}^3$

function, see Figure 16. It can be clearly seen for the investigated ship that for each Froude number a different polynomial fits more suitable to the estimated equivalent damping coefficients (data points). For the smallest Froude number Fn=0.00, a linear+cubic polynomial seems to be the best choice. The damping results for a Froude number of 0.10 can be fitted with a linear+quadratic approach, whereas the largest Froude number 0.19 needs at least a linear+quadratic+cubic polynomial for the estimated data points. The selection of the right polynomial is different for every case and cannot be generalized at least for the presented model. Furthermore, extrapolations should be omitted.

It is recommended to select an approximation by series expansion or interpolation after the analysis of the time series, see Figure 15 – lower chart. A control plot helps to indentify mismatches. Data points can be summarised and averaged before an approximation. This also leads to discrete

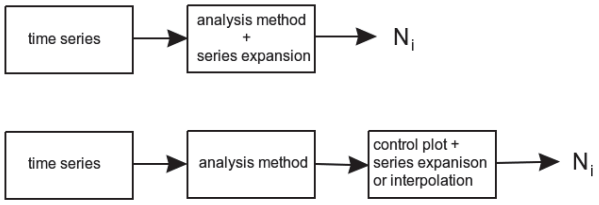

Figure 15 Flow chart of roll damping estimation from time series – general procedure (upper picture), recommended procedure (lower)

distances between data points for a correct approximation.

6. CONCLUSIONS

Different analysis methods for the decay (I) and harmonic excited roll motion (HERM, II) techniques are compared. The focus is set on the accurate estimation of roll damping without additional low-pass filtering and curve fitting. Recommended analysis methods are identified regarding the sensitivity of measurement offsets. These methods are:

- for the *decay technique*: method (D.B), based on the determination of the potential energy in the roll maximum ($\dot{\varphi} = 0$)
- and for the *HERM technique*: method (H.C), based on the determination of the first Fourier coefficient in phase with the roll velocity.

All analysis methods consider non-linear GZ curves of the ship geometry. For a comparison of the damping results for both techniques, a correct estimation of the hydrostatic moment is needed. Therefore, a possibility of using the dynamic test results to estimate the GZ curve during HERM measurements is presented.

Series expansions are often used for time domain simulations to approximate equivalent damping results. The form of series expansion should not be generalized over all Froude numbers, at least for the presented test case.

7. ACKNOWLEDGEMENT

The project was funded by the German Federal Ministry of Economics and Technology under the aegis of the BMWi-project "Best-Rolldämpfung" within the framework program "Schifffahrt und Meerestechnik für das 21. Jahrhundert". The authors would like to thank the cooperation partners in the project: University Duisburg-Essen, Potsdam Model Basin and the DNV-GL. The authors thank also the HSVA for the support during the evaluation of the test results.

8. REFERENCES

26th ITTC, Specialist Committee on Stability in Waves, 2011, "Recommended Procedures – Numerical Estimation of Roll Damping", International Towing Tank Conference, URL January 2015: http://ittc.sname.org.

Bassler, C.C., Reed, A.M. and Brown, A.J., 2010, "Characterization of Energy Dissipation Phenomena for Large Amplitude Ship Roll Motions", Proceedings of the 29th American Towing Tank Conference, Annapolis, MD, USA.

Blume, P., 1979, "Experimentelle Bestimmung von Koeffizienten der wirksamen Rolldämpfung und ihrer Anwendung zur Abschätzung extremer Rollwinkel", Ship Technology Research / Schiffstechnik, Vol. 26, pp. 3-23 (in German).

el Moctar, B., Shigunov, V. and Zorn, T., 2012, "Duisburg Test Case: Post-Panamax Containership for Benchmarking", Ship Technology Research / Schiffstechnik, Vol. 59/3.

el Moctar, B., Kaufmann, J., Ley, J., Oberhagemann, J., Shigunov, V. and Zorn, T., 2010, "Prediction of ship resistance and ship motion using RANSE", A Workshop on Numerical Ship Hydrodynamics, Proceedings, Vol. II, Gothenburg, Sweden.

Gao, Q., Jin, W. and Vassalos, D., 2010, "Simulation of Roll Decay by RANS Approach", A Workshop on Numerical Ship Hydrodynamics, Proceedings, Vol. II, Gothenburg, Sweden.

Handschel, S., Köllisch, N., Soproni, J.P. and Abdel-Maksoud, M., 2012a, "A Numerical Method for the Estimation of Ship Roll Damping for Large Amplitudes", 29th Symposium on Naval Hydrodynamics, Gothenburg, Sweden.

Handschel, S. and Abdel-Maksoud, M., 2014a, "Improvement of the Harmonic Excited Roll Motion Technique for Estimating Roll Damping", Ship Technology Research / Schiffstechnik, Vol. 61/3, pp. 116-130.

Handschel, S., Fröhlich, M., and Abdel-Maksoud, M., 2014b, "Experimental and Numerical Investigation of Ship Roll Damping by Applying the Harmonic Forced Roll Motion Technique", 30th Symposium on Naval Hydrodynamics, Hobart, Tasmania, Australia.

Himeno, Y., 1981, "Prediction of Ship Roll Damping – State of the Art", Report at Univ. of Michigan – Nav. Arch. And Mar. ENgr., USA.

Roberts, J.B., 1985, "Estimation of Nonlinear Ship Roll Damping from Free-Decay Data", Journal of Ship Research, Vol. 29/2, pp. 127-138.

Röös, B., 2009, "Numerische Untersuchung der Rolldämpfung", Diploma Thesis, University Duisburg-Essen (in German).

Salui, K.B., 2004, "A RANS Based Prediction Method of Ship Roll Damping Moment", University Research Presentation Day, University of Glasgow and Strathclyde.

Sarkar, T. and Vassalos, D., 2000, "A RANS-

based technique for simulation of the flow near a rolling cylinder at the free surface", Journal of Marine Science and Technology, Vol. 5.

Schumacher, A., 2010, "Rolldämpfungs-versuche mit dem Modell eines großen Containerschiffes – Teilvorhaben Mat-Roll", Report at Hamburgische Schiffbau-Versuchsanstalt (HSVA), Germany (in German).

Spouge, J.R., 1988, "Non-Linear Analysis of Large Rolling Experiments", Int. Shipbuild. Progr., Vol. 35/403, pp. 271-320.

Sugai, K. and Yamanouchi, Y., 1963, "A Study on the Rolling Characteristics of Ship by Forced Oscillation Model Experiments", Journal of Society of Naval Architects of Japan, pp. 54-66 (in Japanese).

9. APPENDIX

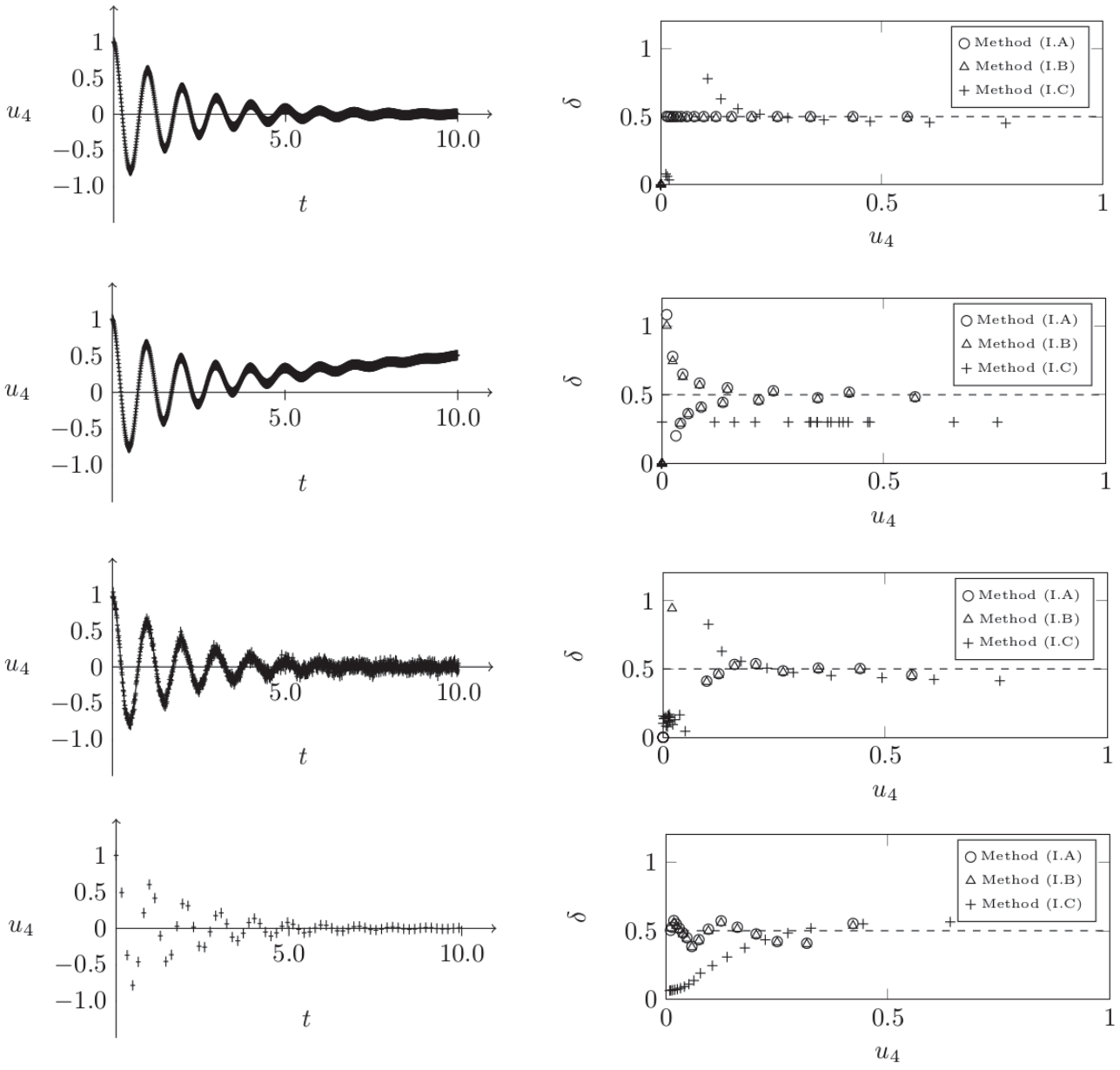

Figure 17 Comparison of methods (D.A), (D.B) and (D.C) – *D is labelled as I in the legends, left column: signal, right column: damping value, dotted line: target damping value* – an undisturbed signal (first picture), signal with white Gaussian noise (second), signal with a large offset (third) and a signal with a lower sampling rate (fourth)

Table 5 Comparison of methods (H.A), (H.B) and (H.C) – *target damping value is 0.5* – for an undisturbed signal, signal with white Gaussian noise, signal with a large offset and a signal with a lower sampling rate

	(H.A)	(H.B)	(H.C)
Undisturbed signal	0.49820	0.50076	0.50103
White Gaussian noise	0.59482	0.49009	0.49160
Large offset	0.52570	0.50076	0.50127
Lower sampling rate	0.32717	0.46653	0.48473